ISSN 1028-334X, Doklady Earth Sciences, 2006, Vol. 406, No. 1, pp. 41–45. © Pleiades Publishing, Inc., 2006.
Original Russian Text © Yu.A. Litvin, V.Yu. Litvin, A.A. Kadik, V.A. Zharikov, 2006, published in Doklady Akademii Nauk, 2006, Vol. 406, No. 1, pp. 83–88.

GEOCHEMISTRY

Formation of Reaction Garnets during Melting of the $MgCO_3$–$CaCO_3$–$NaAlSiO_4$–SiO_2 System at 7.0 GPa

Yu. A. Litvin[1], V. Yu. Litvin[2], A. A. Kadik[2], and Academician of the RAS V. A. Zharikov[1]

Received August 8, 2005

DOI: 10.1134/S1028334X06010119

The formation and evolution of deep-seated carbonatite magmas under the *PT* conditions of diamond formation represent complex physicochemical processes that incorporate multicomponent silicate material of mantle peridotite, strongly compressed carbonate melts, and CO_2 fluids, which possibly represent the products of multiphase plume differentiation [1]. Mobile low-viscosity carbonatite magmas belong to the chemically active forms of deep-seated matter of the dynamic mantle. It has been suggested that the carbonatite magmas contribute to mantle metasomatism as "carbonatite fluids" [2]. They are genetically related to both primary kimberlite melts [3] and parental diamond-forming environments [4]. The chemical and phase evolution of carbonatite melts in mantle are not accessible to direct observations and can be resolved only by high-pressure physicochemical modeling. The amount of carbonatite melts in the Earth's crust is insignificant owing to the thermal decomposition of carbonates during their ascent into the low-pressure zones [5].

Previous experimental studies at 2.5 GPa revealed carbonate–silicate liquid immiscibility in the $CaCO_3$–$NaAlSiO_4$ (nepheline) and $CaCO_3$–$NaAlSi_3O_8$ (albite) joins of the model $CaCO_3$–$NaAlSiO_4$–SiO_2 carbonatite system [6, 7]. Mineralogical evidence for the liquid immiscibility of carbonate and silicate melts was also found in carbonatites of spinel–peridotite facies [8].

The present experimental study considers phase relations in the $MgCO_3$–$CaCO_3$–$NaAlSiO_4$ (nepheline)–SiO_2 system at 7.0 GPa and 1200–1800°C. These parameters are consistent with available geothermal estimations and with the diamond formation conditions in the mantle. Variations of the $MgCO_3/CaCO_3$ and $Na_2O/(Al_2O_3 + SiO_2)$ ratios in deep-seated carbonatite assemblages are reflected in this system. $MgCO_3$ and $CaCO_3$ are representative components of mantle carbonatites, unaltered kimberlites, and carbonatite inclusions in mantle minerals [9] and diamonds [10]. Under mantle pressures, these components, like dolomite $CaMg(CO_3)_2$, are thermally stable and melt congruently. Nepheline $NaAlSiO_4$ and jadeite $NaAlSi_2O_6$ are stable at high pressures [11], whereas albite breaks down to produce jadeite and SiO_2 (quartz or coesite). Jadeite is one of the main components in clinopyroxenes of mantle peridotites and eclogites (omphacite solid solutions). Experiments were carried out in the joins with the carbonate end members (dolomite $CaMg(CO_3)_2$, magnesite $MgCO_3$, and calcite $CaCO_3$) and silicate end members (nepheline $NaAlSiO_4$, jadeite $NaAlSi_2O_6$, and albite $NaAlSi_3O_8$). The latter was represented by a mixture of jadeite $NaAlSi_2O_6$ and SiO_2 at 7 GPa. The $CaCO_3$–jadeite join was chosen for study at 7 GPa in order to accomplish a comparison with chemically similar $CaCO_3$–nepheline and $CaCO_3$–albite systems studied under lower pressures of up to 2.5 GPa [6, 7].

The starting materials were homogeneous mixtures of gels with stoichiometric compositions of nepheline $NaAlSiO_4$, jadeite $NaAlSi_2O_6$, and albite $NaAlSi_3O_8$, as well as chemical reagents of $MgCO_3$, $CaCO_3$, and their mixtures with dolomite stoichiometry $CaMg(CO_3)_2$. The starting mixtures were loaded and sealed in Pt or $Pt_{60}Rh_{40}$ ampules (as a disc 3.5 mm across and 2.5 mm high). The ampules were placed in a pressed isolating mixture of MgO and BN_{hex} (3 : 1, wt %) at the center of tubular resistance furnaces made up of analytical-grade graphite (outer diameter 7.5 mm, inner diameter 6.0 mm, and height 7.2 mm). The furnaces were inserted in the axial cell, which was made of limestone (lithographic stone) from the Algeti area, Georgia. The runs were carried out with the high-pressure anvil-with-hole apparatus for the study of phase equilibrium as in [1]. The pressure and temperature were calibrated, respectively, on the basis of standard Bi sensor and $Pt_{70}Rh_{30}/Pt_{94}Rh_{06}$ thermocouples. The pressure at high temperatures was also corrected with the graphite–diamond equilibrium curve. The pressure and temperature were determined

[1] *Institute of Experimental Mineralogy, Russian Academy of Sciences, Chernogolovka, Moscow oblast, 142432 Russia; e-mail: litvin@iem.ac.ru*

[2] *Vernadsky Institute of Geochemistry and Analytical Chemistry, Russian Academy of Sciences, ul. Kosygina 19, Moscow, 119991 Russia*

Experimental conditions and representative compositions of garnets formed in the $MgCO_3$–$CaCO_3$–$NaAlSiO_4$–SiO_2 system at 7 GPa

Sample no.	Composition, mol %	*T*, °C	τ, min	Phase	Composition (wt %)/f.u.					Total
					Na_2O	MgO	CaO	Al_2O_3	SiO_2	
1316	$Ms_{20}Jd_{80}$	1550	20	Prp	1.74/0.45	26.81/5.37	–	24.89/3.94	46.55/6.25	99.99
1318	$Ms_{20}Ne_{80}$	1550	20	″	0.85/0.23	28.76/5.85	–	25.66/4.10	45.55/6.18	100.85
1317		1400	40	″	0.99/0.26	28.61/5.81	–	26.79/4.30	44.80/6.11	101.19
1326	$Dol_{20}Jd_{80}$	1570	20	Grt	0.47/0.13	13.55/2.78	19.81/3.02	23.73/3.97	42.83/6.09	100.00
1325		1400	40	″	1.35/0.37	6.38/1.34	25.31/3.83	23.00/3.83	41.95/5.92	97.99
1310	$Cal_{20}Ab_{80}$	1550	20	Gros	0.67/0.19	–	34.47/5.72	21.27/3.69	40.18/5.91	98.47
1309		1400	40	″	0.90/0.26	–	36.42/5.85	21.61/3.82	41.22/6.18	100.14
1312	$Cal_{20}Ne_{80}$	1550	20	″	0.83/0.24	–	36.87/5.92	22.17/3.91	39.87/5.97	99.74
1178	$Cal_{50}Jd_{50}$	1350	65	″	1.47/0.44	–	37.77/6.19	21.86/3.98	40.54/6.27	101.68

Note: Carbonates: (Cal) calcite $CaCO_3$, (Dol) dolomite $CaMg(CO_3)_2$, (Ms) magnesite $MgCO_3$; aluminosilicates: (Ab) albite $NaAlSi_3O_8$, (Jd) jadeite $NaAlSi_2O_6$, (Ne) nepheline $NaAlSiO_4$.

with an accuracy of ±0.1 GPa and ±15°C, respectively. The quenching rate was approximately 300°C/s. Samples embedded in epoxy were polished in very fine diamond powder and studied on a CamScan MV2300 (VEGA TS 5130 MM) electron microscope equipped with a Link INCA Energy microprobe at the Institute of Experimental Mineralogy (A.N. Nekrasov and K. V. Van, analysts).

The table shows conditions and results of experiments at 7.0 GPa in binary joins with carbonate end members, represented by $CaMg(CO_3)_2$, $MgCO_3$, and $CaCO_3$; silicate end members, represented by $NaAlSiO_4$(nepheline) and $NaAlSi_2O_6$ (jadeite); and the albitic mixture ($NaAlSi_2O_6$ + SiO_2).

The important pioneering results obtained are as follows.

(1) The melting of carbonate–aluminosilicate systems (aluminosilicate content >50 mol %) is accompanied by a reaction between carbonate and aluminosilicate components, resulting in the formation of pyrope, pyrope–grossular, and grossular garnets. (2) The melting of carbonate-rich systems (carbonate content >50 mol %) produces homogeneous, completely miscible carbonate–silicate melts. Depending on the carbonate end member, liquidus phases are represented by dolomite $CaMg(CO_3)_2$, magnesite $MgCO_3$, or aragonite $CaCO_3$.

The reactions of garnet formation in the studied systems are unusual, since they proceed only after the appearance of carbonate melts in the aluminosilicate-rich charges. No interaction was observed between carbonates and aluminosilicates under subsolidus conditions.

Some features of the reactions of garnet formation in the carbonate–aluminosilicate systems are illustrated in Figs. 1–4.

Figure 1 demonstrates reaction pyrope–grossular garnets formed by way of melting in the $CaMg(CO_3)_2$ (dolomite)–$NaAlSi_2O_6$ (jadeite) system at 7 GPa. Garnet compositions are given in the table. After quenching under high pressure, the samples are transformed into a fine-grained mass of both multicomponent Ca,Mg,Na-carbonate material and carbonate phases (dolomite, magnesite, and aragonite) with occasional coesite and corundum.

Figure 2 demonstrates reaction grossulars obtained by melting in the $CaCO_3$ (calcite)–$NaAlSi_2O_6$ (jadeite) system at 7 GPa at subsolidus temperature. In this sample, one can see three distinct zones within the area under thermal gradient conditions (Fig. 2a). (1) The lower part of the figure includes a low-temperature zone consisting of a subsolidus assemblage of jadeite (dark gray) and Ca-carbonate as aragonite (light gray). This zone shows a distinct convex boundary, which presumably formed during the initial melting of sample and that records the solidus isotherm (about 1350°C). (2) A higher-temperature narrow dark gray zone of mainly jadeite composition is located above the solidus isotherm. This zone formed when mobile and low-viscosity carbonate melts migrated toward the higher-temperature zone, dissolved jadeite along the conduit, and merged into relatively large drops. (3) The uppermost part of the figure shows the highest-temperature (light) zone, consisting of grossular-bearing drops arranged as garlands at a small distance (about 50–100 μm) from the solidus isotherm. Each individual drop typically contains one grossular monocrystal. Such monocrystals make up paler and coarser-grained chains among the fine-grained matrix. Grossular is developed as perfect monocrystals with smooth faces and distinct straight edges (Fig. 2b). Grossular compositions are given in Table 1. After quenching under pressure, the melts are

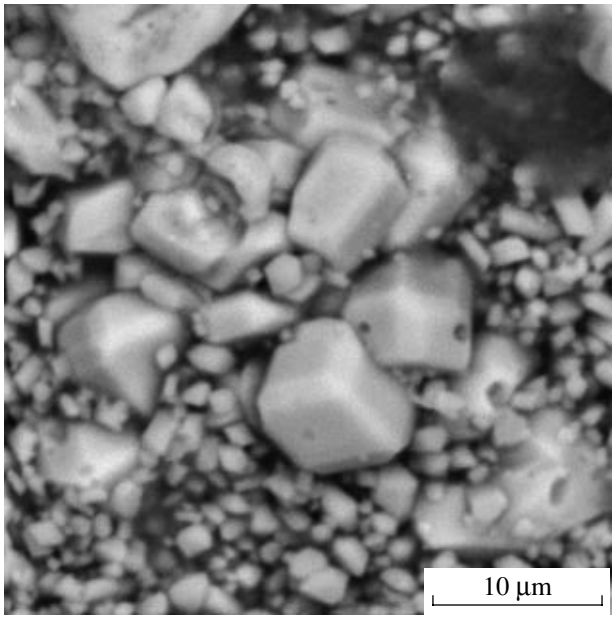

Fig. 1. Reaction pyrope–grossular garnets formed during melting in the $CaMg(CO_3)_2$ (dolomite)–$NaAlSi_2O_6$ (jadeite) system at 7 GPa (sample 2/1326).

transformed into fine-grained dendritic matrix consisting of the Ca–Na carbonate, aragonite, Na_2CO_3, and occasional coesite.

Figure 3 presents reaction pyropes formed in the $MgCO_3$ (magnesite)–$NaAlSiO_4$ (nepheline) system at 7 GPa. It is very important for our understanding of the mechanisms of garnet formation that pyrope grains are overgrown with the Na_2CO_3 shell fragments, which represent the remnants of a quenched melt that produced garnet grains at the late stages of reaction. The groundmass contains corundum.

Figure 4 shows porous zones in the reaction front along the periphery of two garnet formation zones in the $CaCO_3$ (calcite)–$NaAlSi_2O_6$ (jadeite)–SiO_2 (silica) system at 7 GPa (light phase is grossular, while dark gray phase is jadeite with coesite inclusions). One can suggest that such porosity, which was also observed during garnet formation in other systems, is presumably caused by the release of free fluid phase (CO_2) from carbonate melt during quenching. Carbonate–aluminosilicate reactions of the garnet formation occur in the melts not only at solidus temperature, but also at higher temperatures (the limiting temperature in the experiments was 1800°C). The reactions occur exclusively within drops of carbonate melts, in which aluminosilicate components are dissolved. It is interesting that these reactions result in the growth of relatively large garnet monocrystals according to the principle mentioned above: one monocrystal per drop. All stages of garnet growth are traceable in grossular monocrystals under electron microscope. At first, a large skeletal crystal is formed in a carbonate drop. Then the crystal

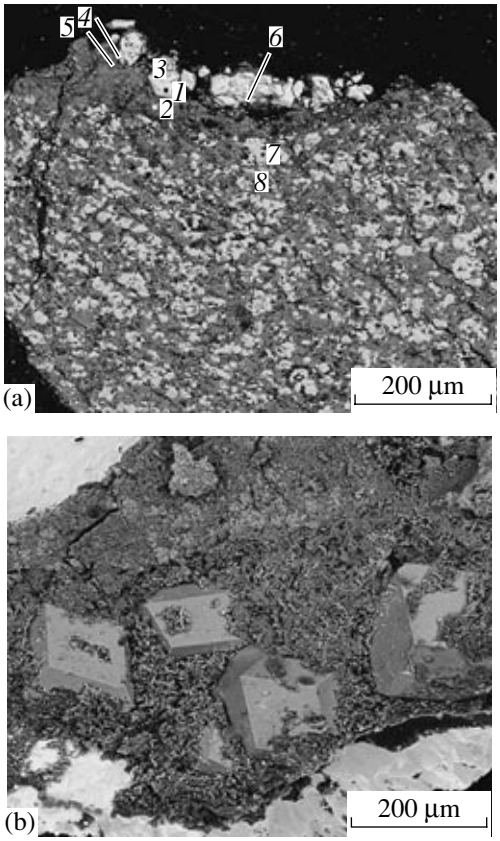

Fig. 2. Reaction grossular garnets formed during melting in the $CaCO_3$ (calcite)–$NaAlSi_2O_6$ (jadeite) system at 7 GPa (sample 2/1178). (a) Subsolidus temperature, (b) group of monocrystals. (*1–8*) Here and in Fig. 3 and 4, sampling points.

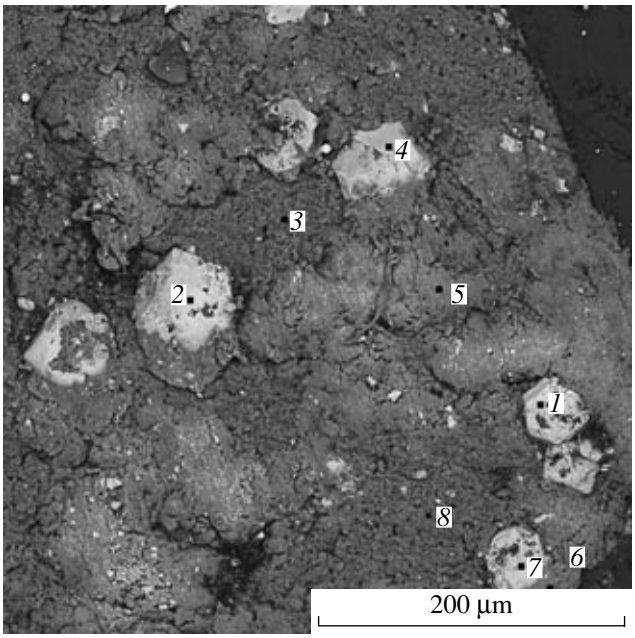

Fig. 3. Reaction pyrope garnets formed during melting in the $MgCO_3$ (magnesite)–$NaAlSiO_4$ (nepheline) system at 7 GPa. Fragments of quenched shells composed of Na_2CO_3 melt are preserved on garnet grains (sample 2/1317).

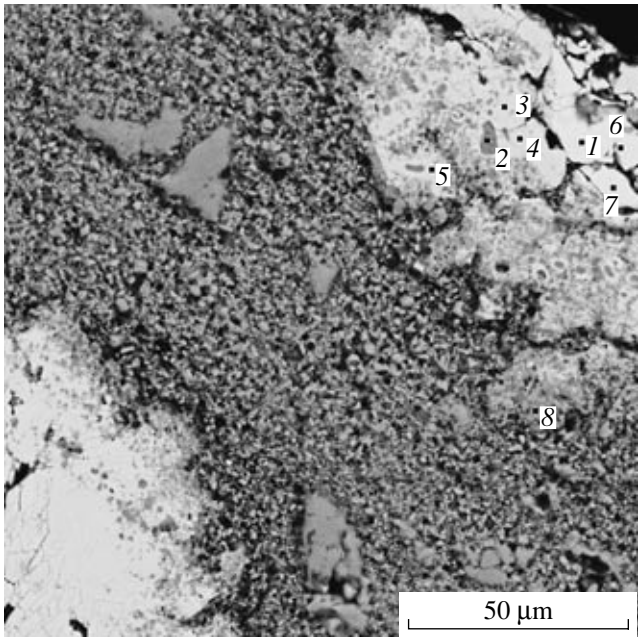

Fig. 4. Porosity related to the probable free fluid phase CO_2 in the reaction front of the grossular garnet formation in the $CaCO_3$ (calcite)–$NaAlSi_2O_6$ (jadeite)–SiO_2 (silica) system at 7 GPa (sample 2/1309).

is transformed into a well-shaped perfect monocrystal (one can observe some such grossular monocrystals in Fig. 2b).

Garnet formation in the carbonate–aluminosilicate melts is exemplified by the reaction with jadeite component:

$$3(Mg, Ca)CO_3\ (melt) + 2NaAlSi_2O_6\ (jadeite, dissolved\ component)$$
$$= (Mg, Ca)_3Al_2Si_3O_{12}\ (garnet, solid\ phase)$$
$$+ Na_2CO_3\ (melt, dissolved\ component)$$
$$+ SiO_2\ (coesite, dissolved\ component)$$
$$+ 2CO_2\ (fluid, dissolved\ component).$$

The reaction of garnet formation in the carbonate–aluminosilicate melts proceeds only in the presence of an excess of aluminosilicate components and continues up to the complete exhaustion of alkaline-earth carbonate components of the melt in each drop. As the reaction proceeds, the proportions of components and alkalinity of initial carbonate melts $(Mg,Ca)CO_3$ vary within the limits of the $(Mg, Ca, Na_2)CO_3$ compositions owing to the formation of alkaline carbonate Na_2CO_3, which becomes a major component of the melts at the final stage of garnet formation. As a result, all alkaline-earth cations are incorporated in garnets, while Na is incorporated in alkali carbonate Na_2CO_3.

There is evidence that strongly compressed CO_2 fluid is also produced during garnet formation in the carbonate–aluminosilicate melts. Like all newly formed components (except garnets), CO_2 fluid remains in a dissolved state and is accumulated in the liquid carbonate phase during the reaction. Pressure within the diamond stability field facilitates this process. It is difficult to observe directly the presence of dense CO_2 fluid in the strongly compressed matter at high pressures and temperatures under conditions of the "closed" high-pressure experiment. Dissolved CO_2 fluid is presumably released from the ampule and lost during the sample quenching. Thus, the formation of CO_2 fluid together with grossular is only evidenced from indirect data (characteristic porosity of experimental phases on the reaction front and balance of components in the carbonate–aluminosilicate reactions).

It should be noted that oxide phases are present as SiO_2 (sometimes corundum appears in the presence of jadeite) in carbonate–aluminosilicate reactions with jadeite and albite, whereas only corundum is present in reactions with nepheline. Their contents reach maximum values at the final stage of garnet formations marked by the exhaustion of $CaMg(CO_3)_2$, $MgCO_3$, and $CaCO_3$, which are sources of Mg and Ca for garnets. Microprobe analyses detected the presence of solid phases of garnet $(Mg, Ca)_3Al_2Si_3O_{12}$, Na_2CO_3, and coesite SiO_2 or corundum Al_2O_3 in reaction products within a drop.

The reactions mentioned above between Mg,Ca-carbonate and aluminosilicate mantle components with the formation of garnet and, possibly, dense CO_2 fluid are of interest, as they represent the possible mechanism of the generation of mantle carbonatite melts with variable contents of dissolved dense CO_2 fluid. During the chemical evolution of carbonatite magmas, with the variation of *PT* conditions toward a significant pressure decrease, the dissolved dense CO_2 can be exsolved from the melt as individual fluid phase. Such a mechanism of CO_2 fluid separation with decrease in pressure and temperature can occur in the ascending kimberlite magmas, leading to an increase of fluid pressure on the overlying rocks, their disintegration, and the explosive emplacement of kimberlites.

In the studied joins of the model $MgCO_3$–$CaCO_3$–$NaAlSiO_4$–SiO_2 carbonatite system, no garnets or dense CO_2 fluid were found in charges with a high content of Mg,Ca-carbonate components. Phase equilibria during their melting are characterized by the formation of homogeneous carbonate–silicate melt with signs of the complete miscibility of carbonate and silicate components. In accordance with the specified compositions of carbonate components, liquidus phases are represented by dolomite, magnesite, or aragonite. It should be noted that chemically similar carbonate–aluminosilicate systems ($CaCO_3$–nepheline and $CaCO_3$–albite, on the one hand, and $CaCO_3$–jadeite, on the other hand) behave differently at relatively low pressures (up to 2.5–3.0 GPa), characterized by carbonate–aluminosil-

icate liquid immiscibility, and at high pressures comparable with diamond formation conditions, which are characterized by complete carbonate–silicate miscibility.

Thus, our experiments revealed the existence of a significant influence of high pressures on the chemical and phase reactions in mantle carbonatite systems. Garnets, the main aluminosilicate minerals in the mantle under conditions of garnet–peridotite facies, participate in the formation of peridotites, pyroxenites, and eclogites. They play an important role in the garnetization of subducted oceanic crust under conditions of mantle dynamics. New reactions between mantle silicate components with the formation of garnets were recently discovered in the high *PT* experiments. For example, pyrope, almandine, and Mg–Fe-garnets are formed in the reaction of forsterite and fayalite with jadeite [12, 13]. Pyrope–grossular garnets are formed in the reactions between diopside and alumina components during high-pressure leucite disproportionation [14]. The present work offers the first report of garnet formation in carbonate–aluminosilicate reactions, presumably, related to the mantle carbonatite magmas and parental diamond-forming environments. Such carbonate–aluminosilicate reactions with the formation of garnets can also be expected for K-aluminosilicates.

At present, concepts of the leading role of parental carbonate–silicate (carbonatite) environments in the genesis of diamond have been elaborated on the basis of mineral and experimental data [15]. Investigations into the issue of the syngenetic formation of diamonds and primary inclusions of minerals, melts, and fluids in them have called the attention of researchers to the garnet formation in carbonate–aluminosilicate melts of mantle carbonatites and parental diamond-forming environments.

ACKNOWLEDGMENTS

This work was supported by the Russian Foundation for Basic Research (project nos. 05-05-64101 and 05-05-64166) and the Program of the Russian Academy of Sciences (no. 27-P) on high-pressure investigations of the Earth and planets.

REFERENCES

1. Yu. A. Litvin, Geol. Geofiz. **39**, 1772 (1998) [Russian Geol. Geophys. **39**, 1761 (1998)].
2. R. L. Rudnick, W. E. McDonough, and B. W. Chappell, Earth Planet. Sci. Lett. **114**, 463 (1993).
3. R. E. Harmer, *Proceedings of 7th Int. Kimberlite Conference, Cape Town, South Africa, 1998* (Cape Town, 1998), p. 302.
4. A. M. Logvinova, O. Klein BenDavid, E. S. Izraeli, *et al.*, *Proceedings of 8th Int. Kimberlite Conference, Victoria, Canada, 2003* (Univ. Victoria, Victoria, 2003), FLA-0025.
5. D. Canil, Earth Planet. Sci. Lett. **18**, 1011 (1990).
6. W. J. Lee and P. J. Wyllie, J. Petrol. **37**, 1125 (1996).
7. W. J. Lee and P. J. Wyllie, Contrib. Mineral. Petrol. **127**, 1 (1997).
8. L. N. Kogarko, C. M. B. Henderson, and H. Pacheko, Contrib. Mineral. Petrol. **121**, 267 (1995).
9. P. Schiano and R. Clocchiatti, Nature **368**, 621 (1994).
10. M. Schrauder and O. Navon, Geochim. Cosmochim. Acta **58**, 761 (1994).
11. Yu. A. Litvin and T. Gasparik, Geochim. Cosmochim. Acta **57**, 2033 (1993).
12. T. Gasparik and Yu. A. Litvin, Eur. J. Mineral. **9**, 311 (1997).
13. V. Yu. Litvin, T. Gasparik, and Yu. A. Litvin, Geochem. Int., Suppl. 1, 100 (2000).
14. O. G. Safonov, Yu. A. Litvin, L. L. Perchuk, *et al.*, Contrib. Mineral. Petrol. **146**, 120 (2003).
15. Yu. A. Litvin and V. A. Zharikov, Dokl. Akad. Nauk **372**, 808 (2000) [Dokl. Earth Sci. **373**, 867 (2000)].